Journal of Education and Science (ISSN 1812-125X)

www.edusj.mosuljournals.com

Equilibrium and Thermodynamic Studies for the Removal of Eriochrome Black T dye from its Aqueous Solutions using Nano Carbon Prepared from Morus Nigra (Mulberry) Stem through two Stages of Carbonization

M. S. Ahmad[(1)], S. O. Ismael[(2)], E. A. S. Al-Hyali[(3)]

[1,2] *Department of Chemistry, College of Science, University of Duhok, Duhok, Iraq*
[3,] *Department of Chemistry, College of Education for Pure Science., University of Mosul, Mosul, Iraq*

Article information

Article history:
Received: April 06, 2024
Accepted: May 26, 2024
Available online: June 01, 2024

Keywords:
Adsorption
Thermodynamics
Isotherms
Eriochrome Black T
Morus Nigra plant

Correspondence:
Maysoon S. Ahmad
maysoon.ahmed@uod.ac

Abstract

In this study, nano-scale activated carbon (NSAC) was synthesized using Morus Nigra (Mulberry) Stem as the precursor material. The carbonization process involved the utilization of KOH, followed by treatment with sodium hydroxide (NSAC-NaOH) to enhance micro-porosity, resulting in higher micro-porous activated carbon. A comprehensive characterization of the material was conducted using various analytical techniques, including Fourier-transform infrared spectroscopy (FT-IR), Brunauer-Emmett-Teller (BET) analysis, field emission scanning electron microscope (FE-SEM), Energy dispersive X-ray spectroscopy (EDX), and X-ray diffraction (XRD). Demonstrated the presence of nano-scale particle size and exceptional porosity. Furthermore, the physical properties of the activated carbon were evaluated, encompassing parameters such as density, humidity, ash content, iodine number, methylene blue pH, and point of zero charge (pH_{PZC}). Adsorption experiments were performed under optimized conditions, with a concentration of Eriochrome Black T (EBT) dye at (100 mg/L), and an adsorbent dose of (0.4g/L), initial concentration(60-110 mg/L), highlighting acidic solutions with a pH of (3.0) as exhibiting superior dye removal capacity, but considering economic factors, the natural pH (5.2) level was determined to be optimal for subsequent experiments, facilitating interaction with EBT dye molecules via electrostatic attraction. Thermodynamic analysis of the adsorption process, conducted within a temperature range of (25–65 ºC), indicated an endothermic nature ($+\Delta H^o$), signifying physical adsorption (ΔH^o < 40 kJ/mol). The negative free energy ($-\Delta G^o$) suggested the spontaneity of the process, while the positive entropy value ($+\Delta S^o$) indicated disorder. Additionally, the Langmuir isotherm model was found to appropriately describe the adsorption behavior of the EBT dye.

DOI: 10.33899/edusj.2024.148527.1445,

1. Introduction

Water is the fundamental essential element crucial for supporting life on our planet, and safeguarding its purity emerges as a pivotal global concern in the modern era. All living beings depend on pure, untainted water for their existence. Despite water covering more than 71% of the Earth's surface, only a small fraction is safe to drink due to various impurities. Even in minimal amounts, the presence of heavy metals, bacteria, and dyes can have detrimental effects on aquatic ecosystems, human health, and the environment[1]. The ongoing degradation of water quality, resulting from the influx of numerous organic, inorganic, and microbiological contaminants, underscores the urgent need for global efforts to combat

water pollution[2]. Given their high toxicity and resistance to degradation, dyes are among the many pollutants present in industrial effluent and should be taken very seriously. Azo dyes are distinguished by the existence of one or more azo functional groups, symbolized by –N=N–, in their molecular arrangement. Removing azo dyes from water is notably tricky due to their considerable resistance to both light and chemical oxidants[3]. Furthermore, the majority of azo dyes are known to be mutagenic and carcinogenic, thus presenting substantial hazards to the health of humans[4]. The anionic EBT dye, categorized as an acidic and azo dye, poses an environmental threat primarily owing to the existence of the N=N bond[5]. Thus, the development of efficient methods for separating hazardous EBT from contaminated streams is crucial. Current studies have focused on utilizing numerous adsorbents to purify wastewater. Selecting the appropriate adsorbent for removing water pollutants relies on various factors, including the concentration and type of pollutant, adsorption capacity, and effectiveness of the pollutant. Moreover, adsorbents need to be non-toxic, affordable, capable of regeneration, and readily accessible. A wide range of adsorbents, including industrial byproducts, agricultural waste, and natural materials, has been utilized in the process of purifying wastewater [1]. Thus, the ongoing pursuit of new, effective, and economical adsorbents remains a crucial objective in sorption research. Activated carbon (AC) represents the most extensively researched and utilized adsorbent materials worldwide. Mainly composed of carbon, these materials exhibit well-developed surface areas and functional groups. Recognized for its unmatched morphological and chemical attributes, AC is acknowledged as a versatile adsorbent. It is employed in the elimination of metal ions and organic compounds from aqueous solutions, as well as in gas removal and storage. With several physical and morphological characteristics, AC can be classified into various forms, including powder, granular, spherical, and fiber-activated carbon[6]. The distinctive characteristics of nano-materials have attracted attention across various disciplines, particularly in studies concerning the adsorption performance of nanoporous carbons. In this study, NSAC was synthesized from Morus Nigra (Mulberry) stems through chemical activation with KOH, introducing a novel adsorbent. Subsequent treatment with sodium hydroxide (NaOH) yielded highly micro-porous activated carbon tailored for the adsorption of EBT. Morus, a common agricultural crop belonging to the Moraceae family, comprises a variety of deciduous tree species commonly referred to as mulberry. It is cultivated in significant quantities in several Asian countries, including Thailand, Korea, China, Japan, India, and the Kurdistan Region of northern Iraq [7]**.** The principal goal of this study is to produce and analyze activated carbon derived from Morus Nigra Stem, followed by modifying its surface through alkaline (NaOH) treatment. These synthesized materials are then used as adsorbents to remove EBT dye from aqueous solutions. The activated carbon possesses a wide range of physical properties, including density, humidity, ash content, iodine number, methylene blue, pH, and pH_{PZC}, which are systematically evaluated. Characterization of the prepared AC, both before and after the adsorption of the anionic dye, is performed using scanning electron microscopy (SEM), energy-dispersive X-ray spectroscopy (EDX), X-ray diffraction (XRD), Brunauer–Emmett–Teller (BET) analysis, and Fourier-transform infrared (FTIR) spectroscopy. Following this characterization, batch adsorption studies are conducted to explore optimal parameters such as adsorbent dose, pH, temperature, contact time, and initial dye concentration. Additionally, various adsorption isotherms and thermodynamics were used.

2. Materials and Methods

2.1. Preparation of nano-scale activated carbon (NSAC) (Adsorbent)

The Morus Nigra (Mulberry) stems underwent drying and were subsequently finely ground into powder form. Mulberry Stem Powder was mixed with potassium hydroxide in a ratio of (1:2.5) (wt:wt). (Mulberry Stem Powder: KOH) using a stainless steel bowl and heated directly over a slow flame using a burner for 90 minutes. After the initial carbonization Process, the temperature was liberated and consistently stirred for three hours to guarantee a complete libation of vapors and gases. The thermal activation process was carried out in a muffle furnace (Nabertherm Lilienthal, Germany, Max 1280 °C) at temperatures of 350 and 550 °C for two hours, respectively, to complete the activation. The mixture was taken off the heat source to purify the activated carbon. To ensure the activated carbon was free from KOH and metal remains, it went through numerous washes using distilled water, effectively eliminating alkaline components. The resulting carbon was refluxed with (10%) hydrochloric acid, and then it was washed several times with distilled water until the removal of any traces of the acid; the product was dried at 110°C and using a sieve size of 75µm and kept in isolation from the air[8].

2.2 Surface treatment of NSAC with NaOH

NSAC was the starting substance for modification through treatment with NaOH, producing NSAC-NaOH. The modification process was carried out to get more NSAC samples with various surface chemical properties while preserving their acceptable morphological qualities. Surface chemical modification's primary objective was to modify the activated carbon's surface acidity and basic to make it easier to add or remove particular surface functional groups. The goal of this modification was to provide the activated carbon with certain catalytic or adsorptive qualities[9]. The procedure began by introducing dry NSAC into a conical flask outfitted with a condenser and heating source. For the oxidation treatment aimed at enhancing the formation of functional groups without surface damage, a 1 M diluted NaOH solution was heated to its boiling point. The oxidation process lasted for 3 hours at this temperature. Following this, the NSAC-NaOH underwent washing and overnight drying at 110 ℃, followed by sieving through 75µm mesh sizes. [10]**.**

2.3. Preparation of EBT Dye (Adsorbate)

EBT, an organic azo dye, shares common characteristics with other azo dyes due to its sulfonate groups and aromatic rings. It displays robust resistance to bacterial or chemical degradation, even at lower concentrations[11]. To prepare a stock solution of the dye with a concentration of 1000 mg/L, 1g of EBT dye was dissolved in a 1L volumetric flask and then diluted with distilled water to the designated volume mark. The stock solution was diluted to get the required concentration for the working solution. Table 1 outlines the general attributes and chemical composition of EBT dye. [12].

Table 1. The general characteristic of the EBT dye

Characteristic	EBT	Chemical structure
General name	Eriochrome Black T	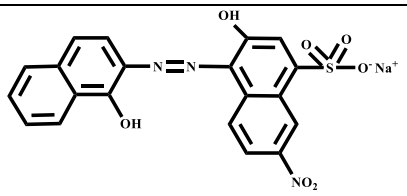
Chemical formula	$C_{20}H_{12}N_3O_7SNa$	
Molecular weight (g mol^{-1})	461.381	
Dye type	Azo dye	
Color type	Brownish black	
Appearance	Powder	
Nature	Anionic	
λmax (nm)	531	

2.4 Characterization of prepared adsorbent

2.4.1. physicochemical properties of the adsorbent:

The precision of experimental characterization for NSAC greatly depends on how samples are prepared. Many measurement methods require careful handling of samples and controlled drying to remove absorbed moisture and gases, ensuring accurate analysis of the adsorbent[13]. NSAC can be evaluated based on its activity and physical properties, including bulk density, moisture content, ash content, iodine number, methylene blue adsorption, pH, and pHpzc. The bulk density[14], moisture Content, and Ash Content [15] were determined according to Eqs. (1,2,3)

$$\text{Bulk density } (g/cm^3) = \frac{\text{Weight of dry sample}}{\text{volume sample}} \quad (1)$$

$$\text{Moisture content } \% = \frac{(m_\circ - m_1)}{m_\circ} \times 100 \quad (2)$$

where: $m_\circ$: the initial mass of AC (g), m_1: mass of AC after drying (g)

$$\text{Ash Content}(\%) = \frac{\text{Weight of Ash produced}}{\text{initial weight of sample}} \times 100 \quad (3)$$

The ASTM D4607-94 method (2006) [16] employs the iodine number as a technique for determining the internal adsorption capacity (mg/g). Meanwhile, the adsorption capacity of methylene blue, represented as q_{MB}, is utilized to evaluate the external capacity (mg/g) of the adsorbent surface [17]. This evaluation involves computations using the Eq. (4)

$$q_{MB}(mg/g) = \frac{C_0 - C_e}{m} \times V \quad (4)$$

Where m = mass of activated carbon in gram V = volume of tested solution in litter C_o= initial concentration of MB dye, Ce= concentration of MB at equilibrium. Finally, the pH [18]and pHpzc [15] of NSAC were measured using a digital (JENWAY 3505 pH Meter).

2.4.2. Surface Characterization

Functional groups on the surface of NSAC and NSAC-NaOH, which are responsible for dye binding before and after adsorption, were investigated using FTIR spectroscopy and recorded by (1800 Shimadzu, Japan spectrophotometer). The determination of the surface area of activated carbons, pore volumes, and pore dimensions was done using the BET method (BEL, BELSORPMINIII, Japan). FE-SEM was used to examine the surface morphology of both AC adsorbents using (TESCAN, MIRA III, Czech). EDX was attached to an FE-SEM to identify the elemental composition of the adsorbent. The crystal structure and phase purity were determined for NSAC using the XRD technique (Philips, PW1730, Holanda, X-ray diffractometer).

2.5 Batch Adsorption Study:

Adsorption experiments were performed in 50-ml conical flasks, each containing 25 ml of EBT dye solution with an initial concentration of (100 mg/L). The solution's natural pH was (5.2), containing 0.01 g of activated carbon. The mixtures were subjected to continuous shaking at 100 rpm using a thermostatic shaker (CAT No SBS40-POWER 1400W) set at 25°C for 60 minutes. Subsequently, they were extracted from the shaker at a particular moment and subjected to filtration using filter paper. A UV-Vis spectrophotometer (model V5100, PIOWAY) at λmax of 531 nm was employed to generate a calibration

curve. That was used to measure the amount of residual solution. Adsorption tests were performed to investigate the effects of adsorbent dose (0.01-0.05 g), beginning solution pH (3–9), contact duration (5–100 min), temperature (25–65 °C), and initial dye concentration (60–110 mg/L) on adsorption isotherm, and thermodynamic properties The equilibrium adsorption capacity of EBT dye, represented as qe (mg/g), and the percentage of dye removed was determined using the following equations: Eqs. (5,6) [19].

$$q_e = \frac{C_0 - C_e}{m} \times V \qquad (5)$$

$$R\,\% = \frac{C_0 - C_e}{C_0} \times 100 \qquad (6)$$

Where $C_\circ$ and C_e are the initial and equilibrium EBT dye concentrations (mg/L), V(L) is the volume of the EBT dye, and m is the activated carbon (g) mass. (q_e) the dye's adsorption capacity at equilibrium mg/g.

2.6 Adsorption Thermodynamic Study:

The thermodynamic properties such as the change in Gibbs free energy (ΔG°), enthalpy (ΔH°), and entropy (ΔS°) for the adsorption process of EBT on NSAC and NSAC-NaOH were determined across the temperature range of 298 to 338 K using the Van't Hoff equation, outlined in Eq. (7). The values of ΔH° and ΔS° were derived from the slope and intercept of the lnK versus 1⁄T plot, depicted in Fig. 12. The calculation of ΔG° was carried out according to Eq. (8) [20].

$$\ln K_c = \frac{\Delta S^\circ}{R} - \frac{\Delta H^\circ}{RT} \qquad (7)$$

$$\Delta G^\circ = -RT \ln k_c \qquad (8)$$

Where K_c is the equilibrium constant and $K_c = C_{ad}/C_e$, $C_{ad}$is the equilibrium dye concentration on the adsorbent (mg/L), C_e is the equilibrium dye concentration in solution mg/L , T is the temperature (Kelvin), and R (8.314 J/mol K) is the gas constant.

2.7 Adsorption equilibrium isotherm Study:

The adsorption equilibrium data were analyzed using two widely employed adsorption isotherm models: Langmuir and Freundlich [21]. The Langmuir isotherm assumes homogeneous adsorption with uniform energy of active adsorption sites, while the Freundlich isotherm assumes heterogeneous surfaces. The linear equations representing Langmuir's and Freundlich's models are described by Eqs. (9,10), respectively.

$$\frac{C_e}{q_e} = \frac{C_e}{Q_{max}} + \frac{1}{K_L \times Q_{max}} \qquad (9)$$

$$\ln q_e = \ln K_F + \frac{1}{n} \ln C_e \qquad (10)$$

Where q_e is the amount of adsorbed dye at equilibrium (mg/g), C_e is the equilibrium concentration of dye in solution mg, Q_{max} is the Langmuir theoretical maximum adsorption capacity mg/g, K_L, K_F, and n are the constants of Langmuir and Freundlich isotherm models, Langmuir isotherm can be depicted with a dimensionless constant separation factor, R_L. The value of R_L shows the adsorption condition as unfavorable (R_L more than 1), liner (R_L = 1), irreversible (RL = 0), and favorable (R_L between 0 and 1**).** $R_L$is obtained from Eq.(11) [21]

$$R_L = \frac{1}{(1 + K_L) \times C_\circ} \qquad (11)$$

Where $C_\circ$ is the maximum initial EBT concentration.

3. Results and discussion

3.1-Adsorbent Characterization

The physicochemical properties of NSAC prepared from Morus Nigra (Mulberry) Stem were determined and presented in Table 2 below:

Table 2. Physico-chemical properties of the NSAC

Adsorbent	% of Moisture	% of Ash	Density mg/g^3	Iodine Number mg /g	Methylene Blue mg /g	pH	pH_{pzc}
NSAC	5.2	2.4	0.0942	852.69	183.32	6.77	6.6

Bulk of Density: The density of NSAC can change depending on the raw material utilized, the activation technique employed, and the properties of the activating agents utilized[22]. Therefore, it is essential to consider bulk density when preparing activated carbon. A low density may indicate greater porosity and surface area, desirable characteristics for many applications[14]. Eq. (1) was applied to calculate the density of the NSAC; it was found to be (0.0942 g/cm^3), considered good when compared to prepared types, and demonstrated high adsorption efficiency.

Moisture content: Moisture content in activated carbon denotes the quantity of water present, and the acceptable range is widely less than 10%. The result shows a moisture content of 5.2%, within the permissible range [23]. As Macky [24] indicated, the presence of moisture in wastewater treatment doesn't impair the efficiency of the adsorbent. Instead, it acts as a diluting agent, necessitating a larger quantity of adsorbent to achieve the desired dry weight. Moisture content does not pose a research or scientific issue, as it can be controlled by employing heat in an environment devoid of air.

Ash content: The ash content of carbon denotes the residual material remaining post-combustion of carbonaceous substances. Various factors, including the chemical composition of the initial components, the temperature during carbonization, and the specific oxidizing agent employed, impact the composition of this residue.[25] Our study indicates an ash content percentage of 2.4%; generally, in commercial settings, the acceptable range for ash content in activated carbon varies from 2% to 10%. A lower ash content is desirable as it contributes to a higher fixed carbon value and enhances the quality of the activated carbon[26]

Iodine Number: The iodine number is commonly used to assess the porosity of activated carbon (AC), often serving as an estimate of surface area for specific types of activated carbons. However, it's important to recognize that the correlation between iodine number and surface area isn't consistently reliable, as it is influenced by factors such as the distribution of pore volume, the type of raw material, operational and processing methods [27]. In our investigation, the iodine number for NSAC was determined to be 852.69 mg/g, surpassing that of commercial samples. This higher iodine value in NSAC is attributed to the presence of a substantial micro-pore structure, which can lead to an enlarged surface area due to the expansion of its pore structure [28].

Methylene blue Adsorption: Adsorption capacity was utilized as a method to evaluate the surface area of AC comparatively. The value of the methylene blue dye's adsorption capacity was confirmed to be 183.32 mg/g, which gives a good indication of a considerable external surface area

FTIR analysis: Additional carbonization process occurred using the NaOH base, a comparison was made between the IR spectrum of the prepared carbon and the modified carbon before and after the adsorption process of the EBT dye .The results showed varying bands in terms of the type and intensity of the bands, as shown in Fig 1. The spectrum of prepared carbon NSAC showed two main bands at 1750 cm^{-1}, which may represent (C=O) or (C=C) bands in aromatic compounds that fall in the range 1450-1600cm^{-1} and the band at 1161 cm^{-1} represents (C-N) or (C-O). Before adsorption, NSAC-NaOH showed new bands that appeared at 3417 cm^{-1}, belonging to a phenolic (O-H) or amino (N-H) group, and a new band that appeared at 1415 cm^{-1}. After the adsorption process of the EBT dye occurred on the NSAC, the results showed a band at 3394 belonging to (O-H) or (N-H). A band at 1573 cm^{-1} may belong to the NO_2 group, and distinctive bands appeared like a distinctive fingerprint.

(a)

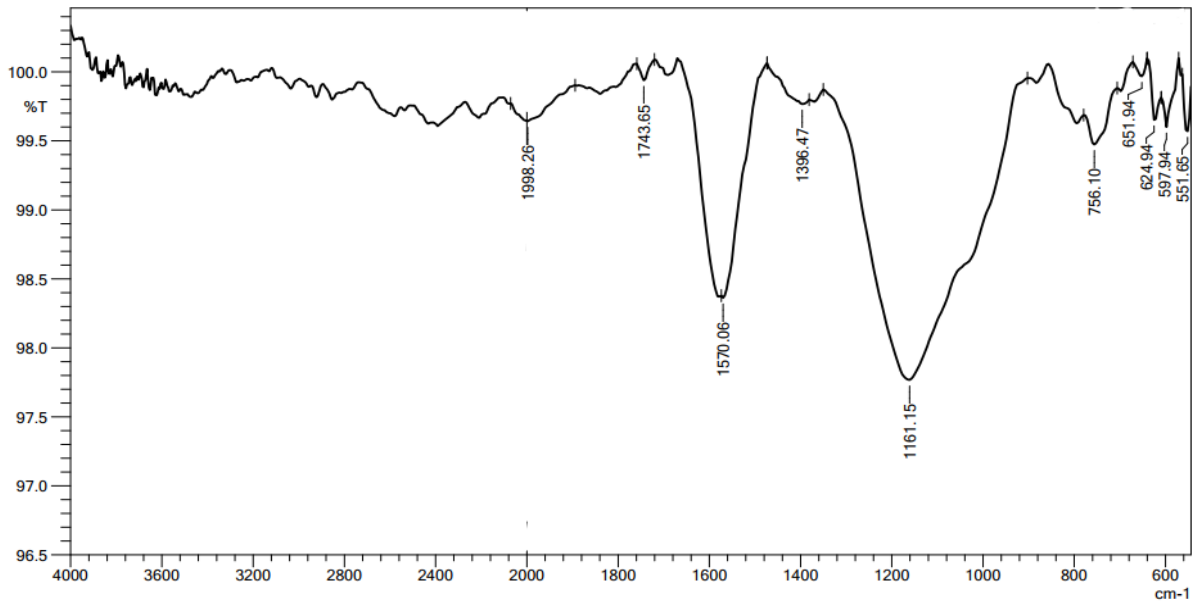

(b)

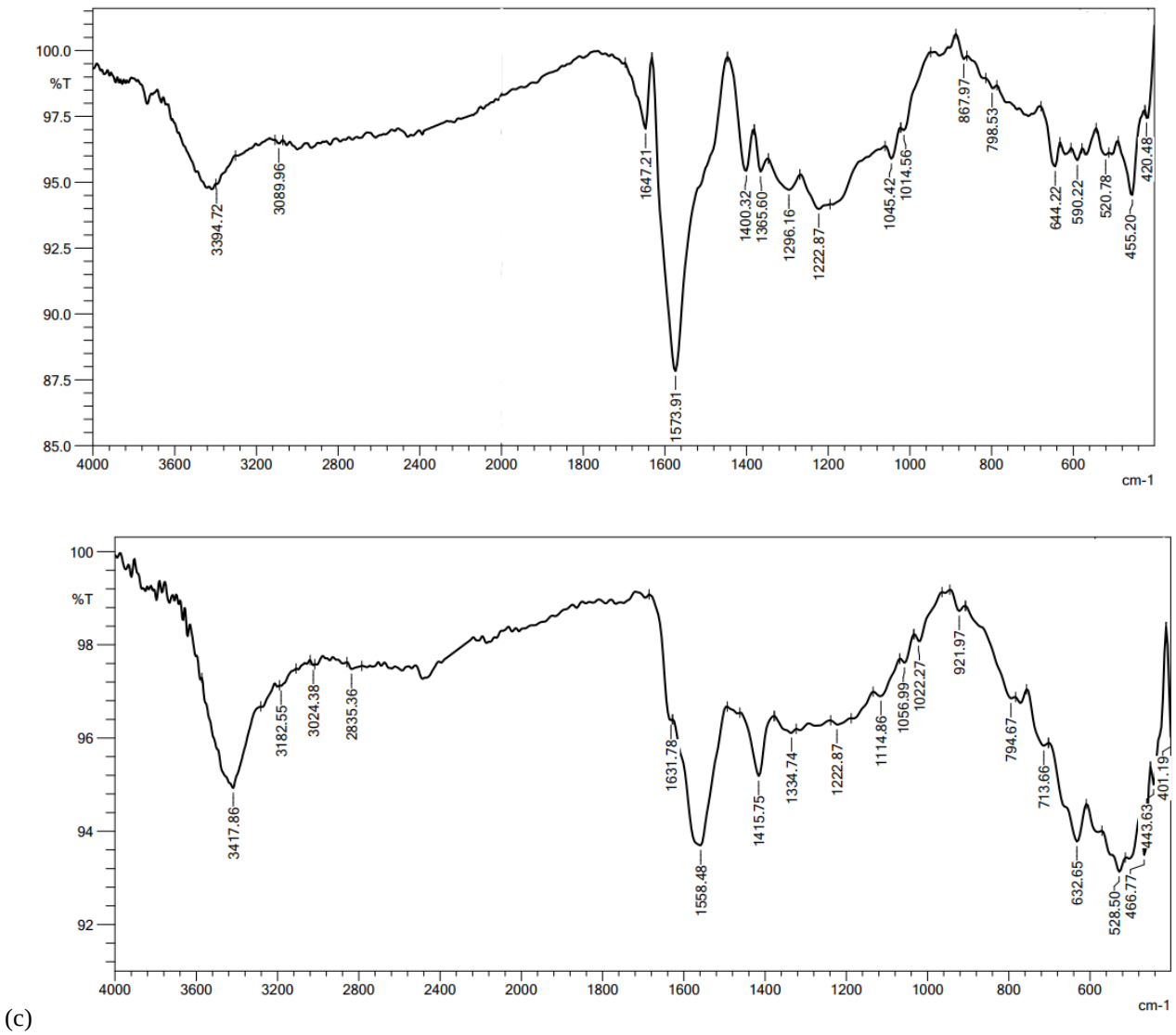

(c)

Figure 1. FT-IR spectra for (a) NSAC before adsorption, (b) NSAC after adoption, and (c) NSAC-NaOH

Surface morphology analysis: Analyzing the surface morphology and confirming the porosity of the adsorbents, samples of the NSAC before and after adsorption underwent examination using SEM (MIRAIII, Tecsan). Fig.2(a) shows an SEM image of NSAC before adsorption. It can be observed that the micrograph of the surface of NSAC shows that its surface has the appearance of sheets with irregular and porous morphology due to chemical activation[29]**.** Fig. 2(b) depicts their spherical form and diameter of 14.70 nm. This confirms that post-adsorption, the porous surface of NSAC was thickened and coated with EBT dye.[30]. The SEM image of NSAC-NaOH after modification is shown in Fig. 2(c). The analysis revealed an increased presence of cavities and a broader pore network on the surface of the AC. Based on the SEM images, it is inferred that chemical activation stimulates the formation of pores and the expansion of pre-existing ones. This observation validates the inherent porous structure of activated carbon [31].

(a)

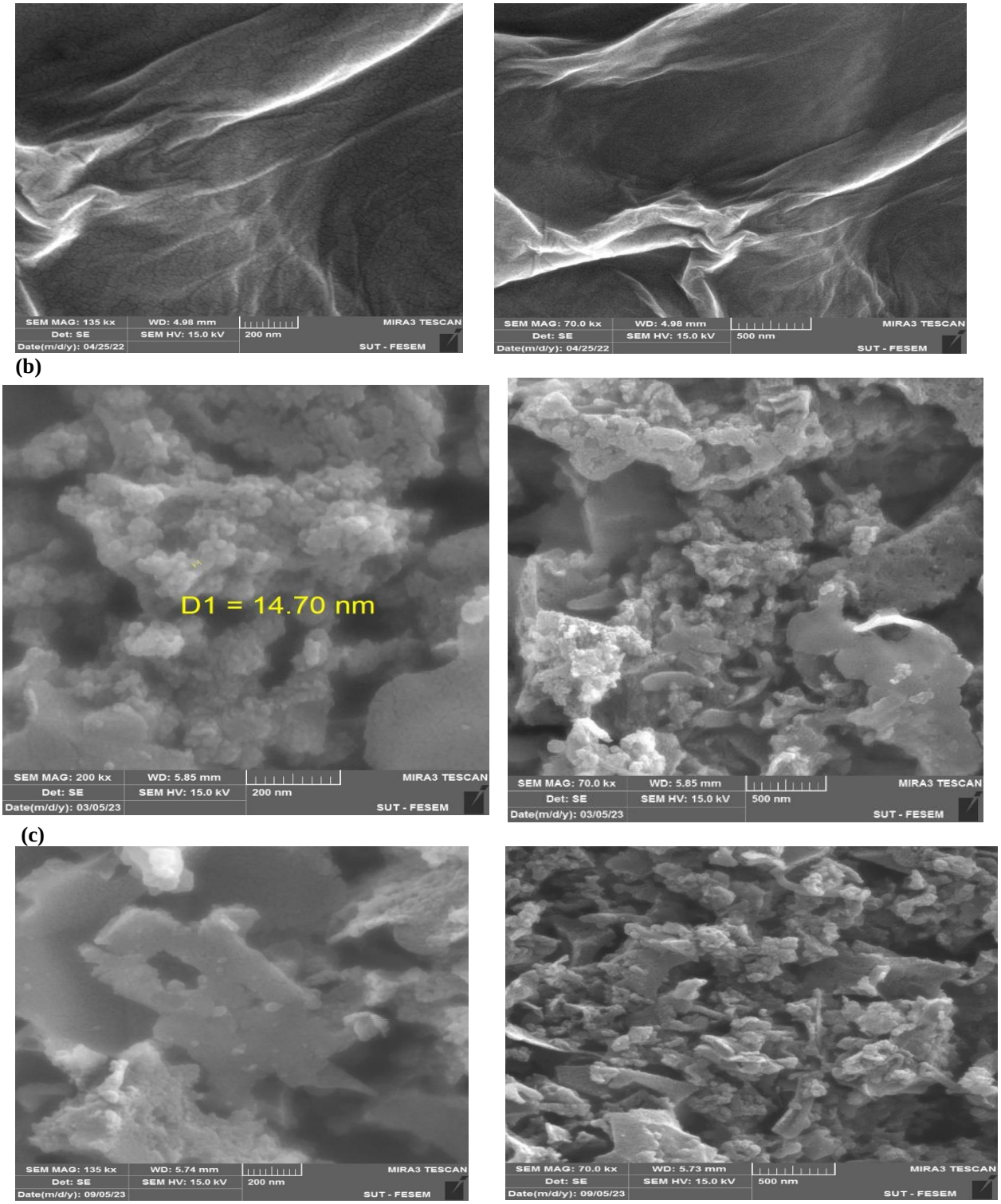

Figure 2. SEM for (a) NSAC before adsorption, (b) NSAC after adoption, and (c) NSAC-NaOH

Specific surface area analysis: Activated carbon's specific surface area is affected by a variety of factors, which include the kin of the activation agent employed, temperature, and the absorption characteristics of the starting material. The temperature of carbonization significantly impacts the formation of pore structure and the overall surface area. Notably,

NSAC-NaOH demonstrates the highest surface area, largely due to its chemical activation with KOH, followed by treatment with NaOH [25]. Table 3 displays the findings of the BET analysis; this high-specific surface area for adsorbents makes it a candidate for use in the adsorption process.

Table 3: BET surface area and porosity of NSAC and NSAC-NaOH.

Adsorbent	BET Surface area m^2 /g	Langmuir surface area m^2 /g	Pore Size cm^3/g	Pore volume cm^3/g	Average Particle size nm
NSAC	448.25	407.24	0.6009	102.99	5.3622
NSAC-NaOH	462.59	518.08	0.5495	106.28	4.7517

Elemental composition analysis: EDX analysis was conducted on NSAC to ascertain the percentage weight of chemical compositions present on the surface, utilizing an X-ray diffractometer (PW1730, Philips, Netherlands). The results, illustrated in Fig. 3, reveal that the material consists of C: 86% and O: 13.4%, with carbon and oxygen being the predominant elements. This substantiates the organic nature of the NSAC adsorbent[32].

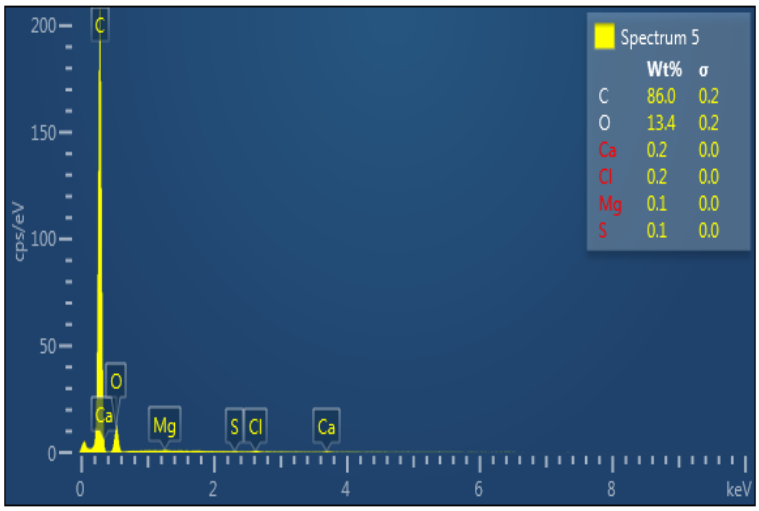

Figure 3. EDX images of NSAC

Crystalline structure analysis: Structural assessment was performed through powder XRD investigations, a method beneficial in discerning the crystalline or amorphous attributes of materials. Crystalline samples manifest sharp peaks, whereas amorphous ones present a solitary broad diffused peak. The XRD graph for NSAC is illustrated in Fig. 4. Evaluation of the XRD results for NSAC confirms its amorphous quality, as indicated by the absence of sharp peaks [31].

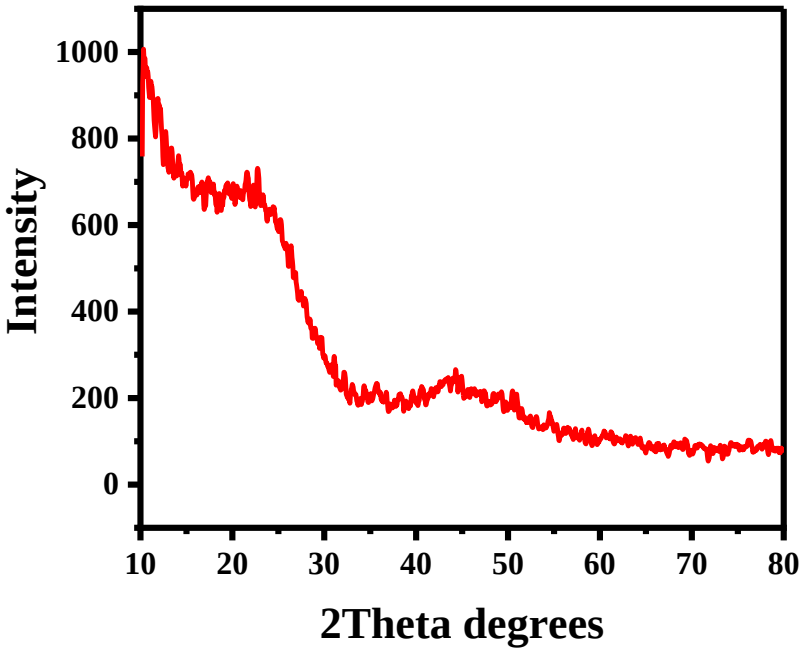

Figure 4. XRD image of NSAC

3.2. Adsorption study in batch mode

3.2.1 Effect of Adsorbent dose

A sequence of experiments was executed to evaluate the impact of adsorbent quantity on EBT removal efficiency and determine the optimal loading of adsorbent. The sample volume was adjusted while keeping all other experimental conditions consistent[33]. The quantity of adsorbent ranged from 0.01 g to 0.05 g while maintaining a constant volume of dye solution (25 ml). As depicted in Fig. 5, the removal efficiency of EBT dye rose from 74.121% to 91.973% as the adsorbent dose increased from 0.01 g to 0.03 g, reaching its maximum. However, this juncture marked the sole significant improvement in adsorption yield. This enhancement can be ascribed to the availability of abundant adsorption sites and increased surface area with higher quantities of adsorbent. Furthermore, lower concentrations of adsorbent resulted in reduced spatial hindrance in the molecular structure of EBT dye, leading to enhanced interactions during the initial stages of adsorption [2]. Taking economic factors into consideration, it was established that an adsorbent dose of 0.01 g of NSAC per 25 ml of dye solution was the optimal choice for future experiments.

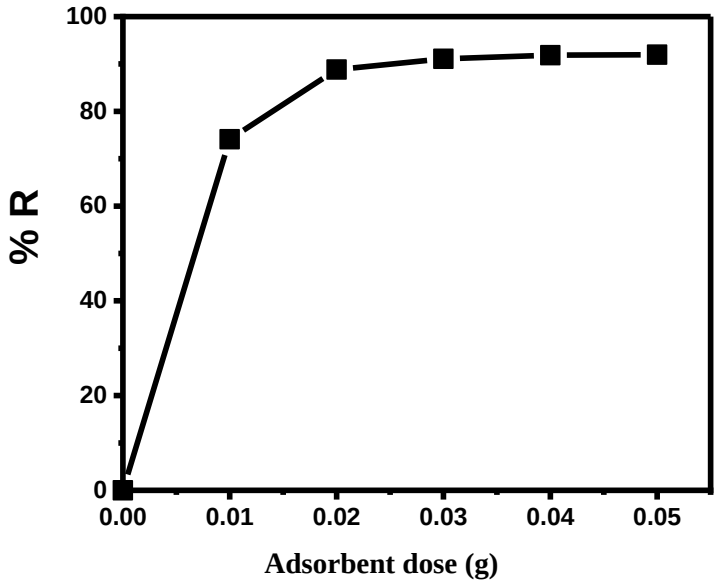

Figure 5. Effect of adsorbent dose NSAC on EBT dye adsorption.

3.2.2. Effect of pH:

Numerous investigations have utilized economical adsorbents derived from agricultural waste to facilitate the absorption of basic dyes under neutral pH conditions. However, addressing the elimination of anionic dyes in such scenarios poses challenges due to the presence of negatively charged functional groups within these adsorbents, leading to electrostatic repulsion between the surfaces of the adsorbents and the anionic dyes. Although substantial dye absorption has been noted at acidic pH levels, this strategy is not viable at the commercial level due to the need for chemical adjustment of the solution's pH. Thus, the main objective of this study was to develop an adsorbent capable of efficiently adsorbing anionic dyes in both single- and multi-component systems at a neutral pH [34]. The results indicate that NSAC and NSAC-NaOH demonstrate high adsorption rates for EBT dye within the acidic pH range, rendering them effective for dye removal through adsorption. The notable removal efficiency at pH=3 is due to the functional groups of the adsorbents' protonated surface. In the case of NSAC, a consistent decrease in EBT dye removal percentage is observed as pH increases from 3 to 9 (Fig. 6(a)). Conversely, for EBT adsorption on NSAC-NaOH (Fig. 6(b)), the removal percentage remains relatively constant within the pH range of 4 to 7. However, at pH levels exceeding 7, a significant decline was observed in the percentage of EBT removal. This decrease implies the existence of OH- ions, which could potentially compete with EBT anions, resulting in a decrease in removal efficiency. The pH_{PZC} of NSAC residues was determined using the solid addition method and was found to be 6.6 (Fig. 6(c)). This implies that when pH levels fall below 6.6, the NSAC surface becomes positively charged and can attract anionic species. Conversely, if pH levels rise above 6.6, the surface becomes negatively charged, potentially leading to competition with anionic species due to electrostatic repulsion. The increased efficacy in eliminating EBT dye under acidic pH conditions is attributed to the formation of a positive charge on the surface functional groups of the adsorbent. This positive charge facilitates electrostatic attraction between the positively charged adsorbent surface and the anionic dyes. Conversely, when the adsorbent surface becomes negatively charged, electrostatic repulsion arises between the anionic dyes and the sorbent surface, resulting in a decrease in adsorption capacity. Similar trends have been observed in the adsorption of CR on bio-based sorbents. [35].

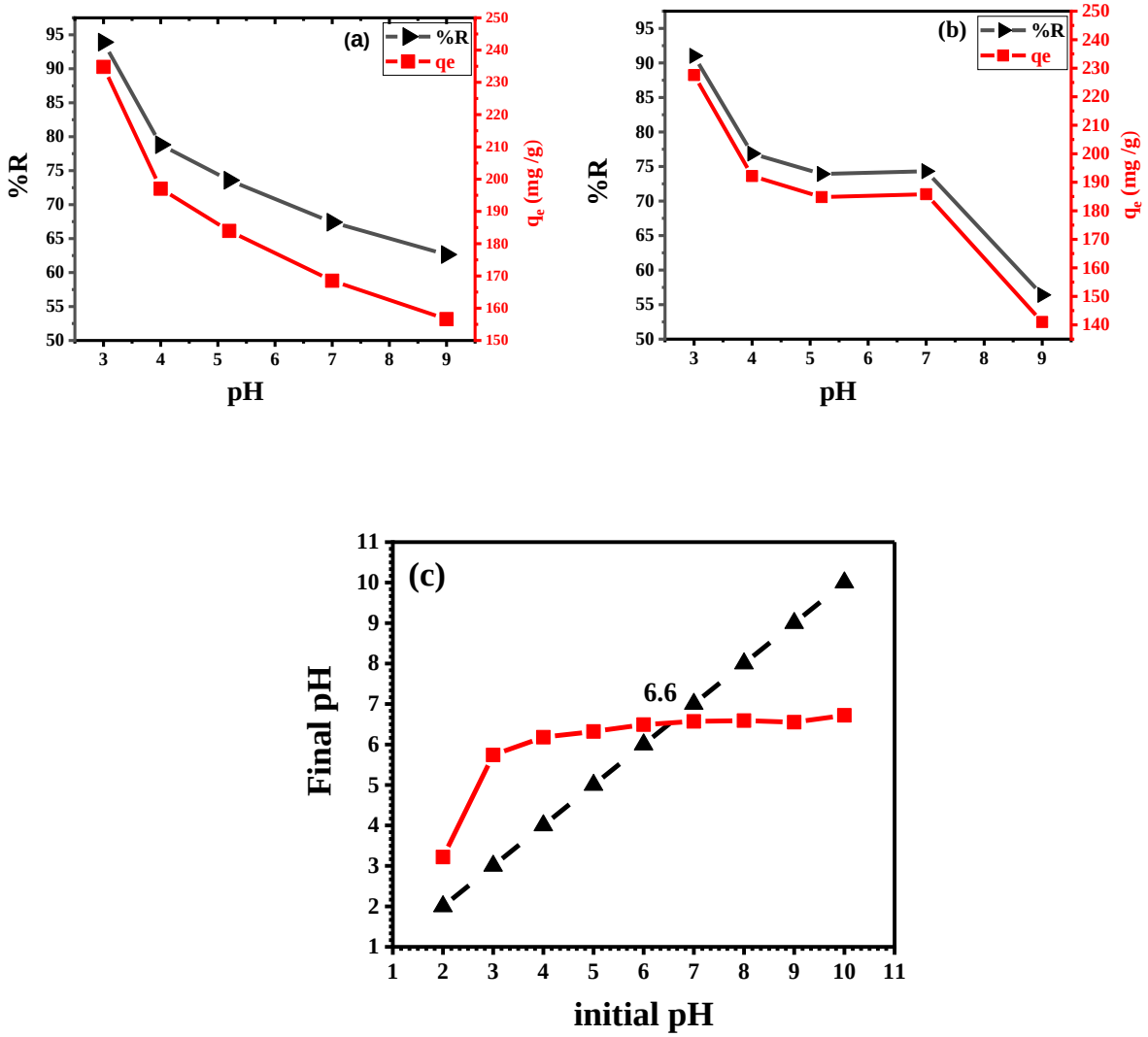

Figure 6. Effect of pH on the %R and qe of EBT dye adsorption on (a) NSAC, (b) NSAC-NaOH, and (c) PZC of NSAC.

3.2.3. Effect of contact time

To evaluate the time required for the adsorption of dye, the effect of contact time on EBT removal percentage was analyzed. As depicted in Fig. 7, both NSAC and NSAC-NaOH showed a rapid increase in dye removal within the first 5 minutes, reaching maximum efficiency within 30 minutes. This swift absorption is credited to the rapid bonding of dye molecules to the surface of the adsorbent, facilitated by the abundance of available sites on the NSAC surface. Subsequently, after reaching a plateau until 80 minutes, the stabilization of adsorption values suggests equilibrium was attained. The adsorption sites gradually being saturated with EBT molecules over time, the elimination of EBT happened more slowly. [36].

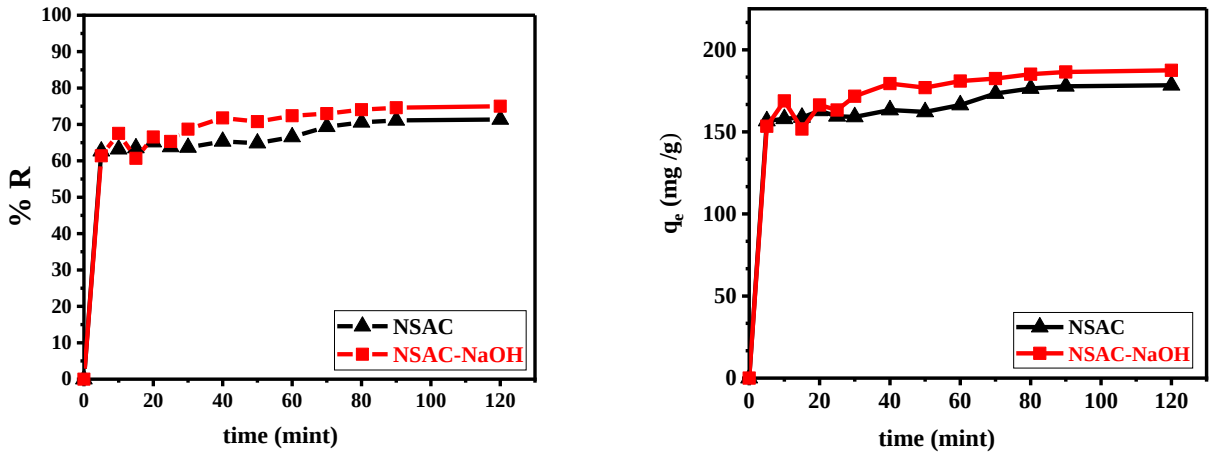

Figure 7. Effect of contact time on the adsorption of EBT on NSAC and NSAC-NaOH at 25 ℃

3.2.4. Effect of initial concentration

Fig. 8 demonstrates how the initial dye concentration affects the adsorption process. The removal percentage (%R) declined from 78.904% to 58.963% for NSAC and from 81.7005% to 68.359% for NSAC-NaOH, respectively. In the lower dye concentration range of 60 to 110 mg/L, the removal efficiency increased due to the availability of active sites on the surface necessary for adsorbing dye molecules. However, as the dye concentration continued to increase, the removal efficiency decreased because the active sites of the adsorbent became saturated, allowing dye molecules to re-enter the liquid phase [37]. On the other hand, the adsorption capacity increased from 118.356 to 162.148 mg/g for NSAC and from 122.550 to 187.987 mg/g for NSAC-NaOH, respectively, as the initial concentration of EBT aqueous solution increased. This increase is attributed to the saturation of active sites at higher EBT dye concentrations. Higher concentrations of EBT in the solution drive a greater mass flow from the liquid phase to the solid phase. This is due to the concentration disparity between the surface of the adsorbent and the EBT in the solution. As the EBT concentration increases, this disparity becomes more pronounced, leading to increased movement of EBT molecules toward the adsorbent surface. This intensified mass transfer enhances adsorption efficiency and boosts the adsorption capacity. However, there is a limit to this phenomenon. Once the active sites on the adsorbent surface are fully saturated, further increases in EBT concentration in the solution do not result in additional adsorption. At this stage, available active adsorption sites are occupied by EBT molecules, making it impossible for the adsorbent to remove any more EBT dye from the solution.[38].

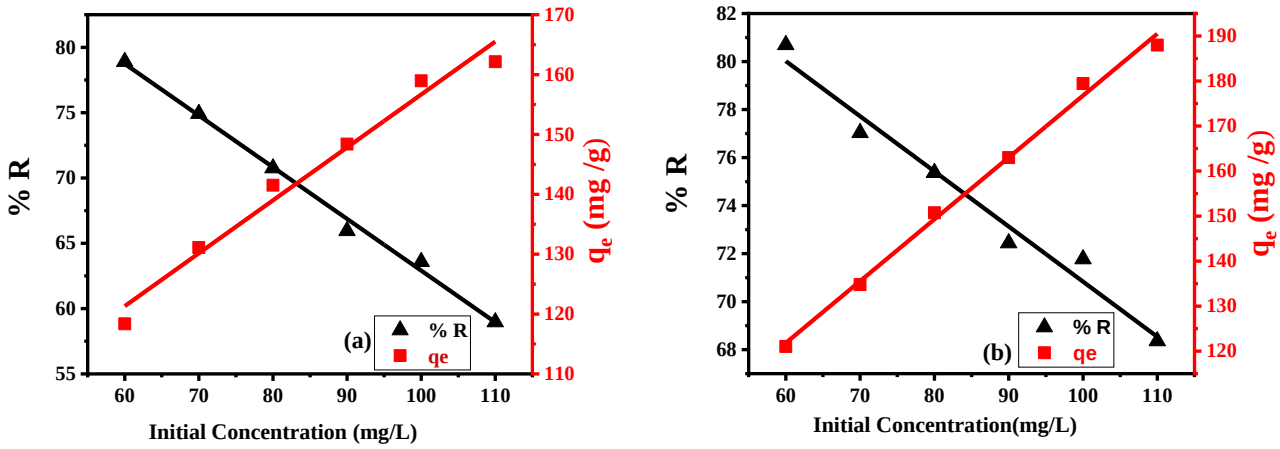

Figure 8. Effect of Initial concentration on the adsorption of EBT on (a) NSAC and (b) NSAC-NaOH at 25 ℃

3.3. Adsorption equilibrium isotherm:

Figs. 9 and 10 illustrate the application of Langmuir and Freundlich adsorption isotherms for EBT on NSAC and NSAC-NaOH, respectively. Table 4 lists the parameters that define both isotherm models. When compared to the Freundlich isotherm, the Langmuir isotherm exhibits the highest maximum adsorption capacity and correlation coefficient (R^2). This indicates a strong correlation between EBT adsorption and the Langmuir model, suggesting a uniform monolayer type of adsorption with consistent adsorption energies; this difference is likely attributed to the uniform distribution of active sites on the surface of the adsorbent. The R_L values for the data in this study range between 0 and 1, implying favorable adsorption of EBT on the adsorbent[21]. Values of n greater than 1 or between 1 and 10 This suggests that the physical adsorption process. This implies that the adsorption bond weakens and is primarily driven by van der Waals forces.

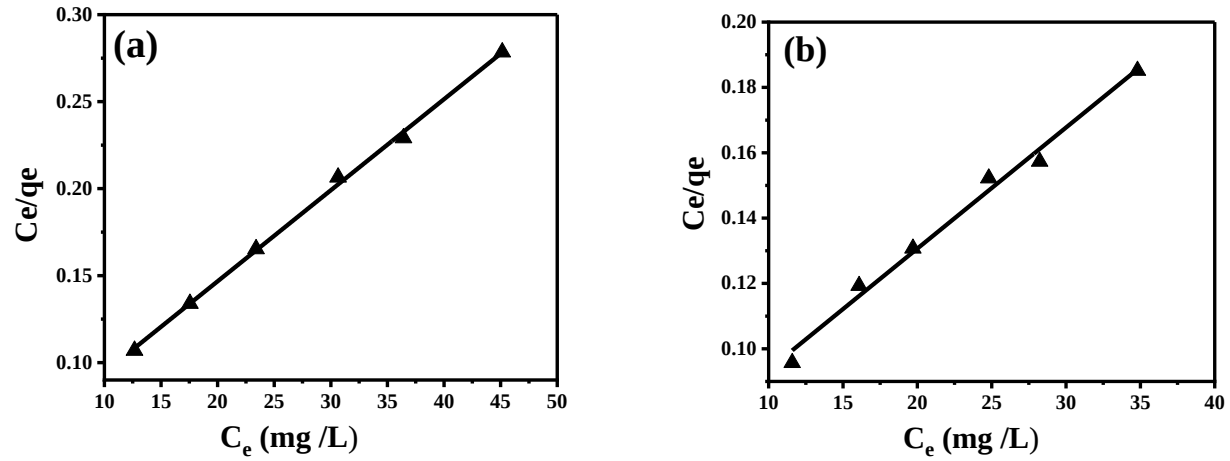

Figure 9. Adsorption Langmuir isotherm of EBT on (a) NSAC and (b)NSAC-NaOH at 25℃

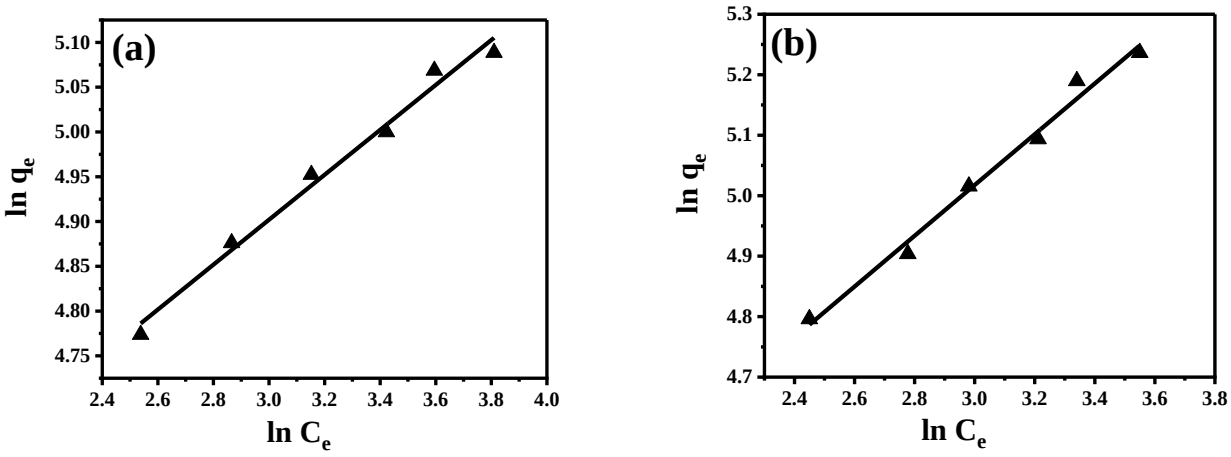

Figure 10. Adsorption Freundlich isotherm of EBT on (a) NSAC and (b)NSAC-NaOH at 25℃

Table 4. Langmuir and Freundlich isotherm constants for the adsorption of EBT on NSAC, NSAC-NaOH at 25 ℃

Adsorbent	Langmuir constant				Freundlich constant		
	Q_{max}(mg/g)	K_L(L/mg)	R_L	R^2	K_F(mg /g)	n	R^2
NSAC	192.308	0.124	0.075	0.9984	63.396	3.986	0.9860
NSAC-NaOH	270.270	0.065	0.133	0.9891	42.888	2.383	0.9880

3.4. Adsorption Thermodynamic Study

Analyzing the thermodynamics of an adsorption method establishes the spontaneity of the process and offers insights into energy alteration. Table (5) indicates that the (ΔG°) values at all selected temperatures are negative, which confirms that the adsorption of EBT dye onto NSAC and NSAC-NaOH is a spontaneous process. The spontaneity increases with increasing temperature, indicating the process's feasibility and favorability at elevated temperatures[39]**.** The positive values of standard enthalpy change (ΔH°) indicate an endothermic lean in the adsorption process, implying the absorption of heat energy from the environment and heat transfer into the system. This is linked to the finding that as temperature rises, adsorption capacity increases.[31]. Furthermore, the value of enthalpy changes for eliminating EBT of less than 20 kJ/mol implies that the primary mechanism for EBT adsorption onto the AC involves physical interactions, specifically electrostatic interactions or van der Waals forces [38]. Moreover, the positive (ΔS°) value signifies an elevation in disorderliness at the interface between the solid and liquid phases during the sorption process, a phenomenon commonly observed in physical sorptionFig.11 shows how temperature fluctuations affect the removal efficiency of EBT.

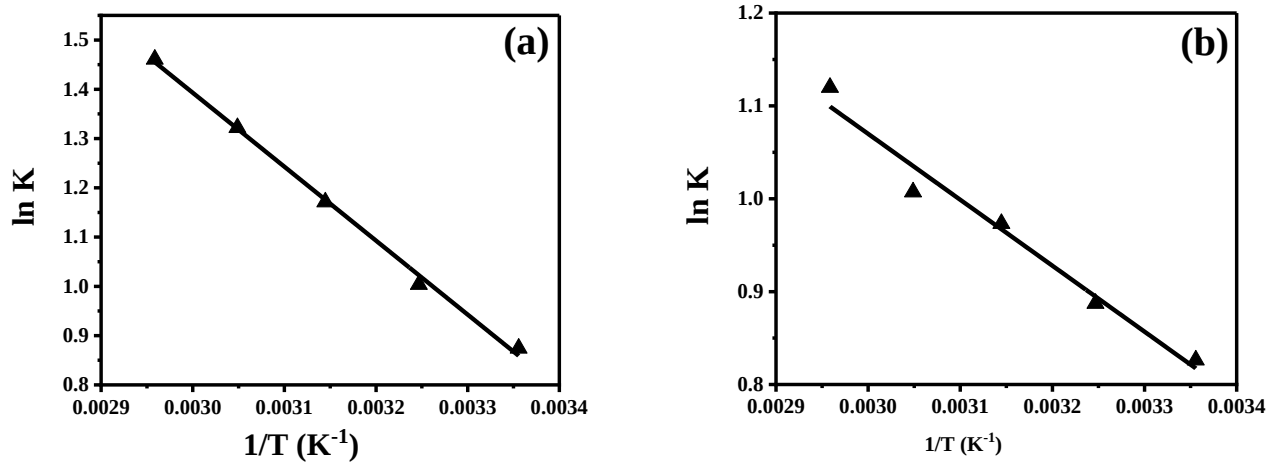

Figure 11. Van't Hof plot of the adsorption of EBT onto (a)NSAC and (b) NSAC-NaOH at different temperatures

Table 5. Thermodynamic parameters for the adsorption of EBT dye onto NSAC, NSAC-NaOH at various Temperatures

			ΔG° kJ/mol				
Adsorbent	ΔH° kJ./mol	ΔS°J/mol. K	**25**℃	**35**℃	**45**℃	**55**℃	**65**℃
NSAC	14.081	54.31	-2.032	-2.562	-3.236	-3.639	-4.193
NSAC-NaOH	5.904	26.606	-2.047	-2.272	-2.573	-2.747	-3.147

4. Conclusion:

This research investigated the synthesis of NSAC and its carbonization using KOH, followed by modifying NSAC surface chemistry to produce NSAC-NaOH. This involved chemically oxidizing the surface to introduce functional groups like carboxylic acid and amine, aiming to enhance AC's adsorption potential for various pollutants in water and wastewater. The method was observed to impact the carbon's pore structure to varying degrees. Typically, treating AC with a base leads to increased adsorption of anionic compounds in water. In alkaline solutions, it was anticipated that OH ions would interact with AC's surface functional groups, thereby improving the adsorption of organic species, such as phenol, from water. Overall, under alkaline conditions, OH ions were expected to react with AC's surface functional groups, creating a more positive charge on the activated carbon surface, which facilitated the adsorption of negatively charged species from water. An investigation into the ideal adsorption conditions, encompassing factors such as adsorbent dosage, contact time, temperature, initial concentration, and solution pH. The Langmuir isotherm equations best represented the equilibrium data. EBT adsorption was identified as spontaneous and endothermic between 298 and 338 K based on measured thermodynamic variables. A newly synthesized activated carbon NSAC derived from Mulberry stem emerged as a cost-effective and efficient adsorbent, highlighting its potential in mitigating industrial waste contamination, particularly in dye removal from water sources.

5. Acknowledgment

The authors express their sincere gratitude to the "Department of Chemistry, College of Science, University of Dohuk" for their assistance, which has been essential in ensuring the successful culmination of this research undertaking.

6. References:

[1] N. B. Singh, G. Nagpal, S. Agrawal, and Rachna, “Wat_A Reviewer purification by using,” *Environmental Technology and Innovation*, vol. 11. pp. 187–240, 2018.

[2] A. Verma, S. Thakur, G. Mamba, R. K. Gupta, P. Thakur, and V. K. Thakur, “Graphite modified sodium alginate hydrogel composite for efficient removal of malachite green dye,” *Int. J. Biol. Macromol.*, vol. 148, pp. 1130–1139, 2020.

[3] U. Baig, M. K. Uddin, and M. A. Gondal, “Removal of hazardous azo dye from water using synthetic nano adsorbent: Facile synthesis, characterization, adsorption, regeneration and design of experiments,” *Colloids Surfaces A Physicochem. Eng. Asp.*, vol. 584, p. 124031, 2020.

[4] S. Benkhaya, S. M’rabet, and A. El Harfi, “Classifications, properties, recent synthesis and applications of azo dyes,” *Heliyon*, vol. 6, no. 1, 2020.

[5] G. A. Haghighat *et al.*, “Zeolitic imidazolate frameworks (ZIFs) of various morphologies against eriochrome black-T (EBT): optimizing the key physicochemical features by process modeling,” *Colloids Surfaces A Physicochem. Eng. Asp.*, vol. 606, p. 125391, 2020.

[6] M. C. Silva *et al.*, “H3PO4–activated carbon fibers of high surface area from banana tree pseudo-stem fibers: adsorption studies of methylene blue dye in batch and fixed bed systems,” *J. Mol. Liq.*, vol. 324, p. 114771, 2021.

[7] S. Siraorarnroj, N. Kaewtrakulchai, M. Fuji, and A. Eiad-ua, “High performance nanoporous carbon from mulberry leaves (Morus alba L.) residues via microwave treatment assisted hydrothermal-carbonization for methyl orange adsorption: Kinetic, equilibrium and thermodynamic studies,” *Materialia*, vol. 21, p. 101288, 2022.

[8] E. . Z. SULYMAN, S. H. SEDEEQ, R. A. S.- ALDEEN, and E. Q. HAMMADI, “Study the Specifications of Activated Carbon Prepared From Avocado Seeds Using Carbonation and Chemical Activation,” *MINAR International Journal of Applied Sciences and Technology*, vol. 4, no. 1. pp. 01–79, 2022. doi: 10.47832/2717-8234.10.7.

[9] M. Liu and C. Xiao, “Research progress on modification of activated carbon,” in *E3S Web of Conferences*, EDP Sciences, 2018, p. 2005.

[10] J. W. Shim, S. J. Park, and S. K. Ryu, “Effect of modification with HNO3 and NaOH on metal adsorption by pitch-based activated carbon fibers,” *Carbon*, vol. 39, no. 11. pp. 1635–1642, 2001. doi: 10.1016/S0008-6223(00)00290-6.

[11] F. El Mansouri *et al.*, “Efficient Removal of Eriochrome Black T Dye Using Activated Carbon of Waste Hemp (Cannabis sativa L.) Grown in Northern Morocco Enhanced by New Mathematical Models,” *Separations*, vol. 9, no. 10. 2022. doi: 10.3390/separations9100283.

[12] G. Zeydouni *et al.*, “Eriochrme black-T removal from aqueous environment by surfactant modified clay: equilibrium, kinetic, isotherm, and thermodynamic studies,” *Toxin Rev.*, vol. 38, no. 4, pp. 307–317, 2019, doi: 10.1080/15569543.2018.1455214.

[13] C. Bläker, J. Muthmann, C. Pasel, and D. Bathen, “Characterization of Activated Carbon Adsorbents – State of the Art and Novel Approaches,” *ChemBioEng Rev.*, vol. 6, no. 4, pp. 119–138, 2019, doi: 10.1002/cben.201900008.

[14] M. A. Yahya, Z. Al-Qodah, C. W. Z. C. W. Ngah, and M. A. Hashim, “Preparation and characterization of activated carbon from desiccated coconut residue by potassium hydroxide,” *Asian J. Chem.*, vol. 27, no. 6, pp. 2331–2336, 2015, doi: 10.14233/ajchem.2015.18804.

[15]G. Y. Abate, A. N. Alene, A. T. Habte, and D. M. Getahun, "Adsorptive removal of malachite green dye from aqueous solution onto activated carbon of Catha edulis stem as a low cost bio-adsorbent," *Environ. Syst. Res.*, vol. 9, no. 1, 2020, doi: 10.1186/s40068-020-00191-4.

[16]ASTM, "Standard Test Method for Determination of Iodine Number of Activated Carbon 1," *ASTM Int.*, vol. 94, no. Reapproved, pp. 1–5, 2006, [Online]. Available: http://compass.astm.org.acces.bibl.ulaval.ca/download/D4607.6656.pdf

[17]F. Raposo, M. A. De La Rubia, and R. Borja, "Methylene blue number as useful indicator to evaluate the adsorptive capacity of granular activated carbon in batch mode: Influence of adsorbate/adsorbent mass ratio and particle size," *J. Hazard. Mater.*, vol. 165, no. 1–3, pp. 291–299, 2009.

[18]D. A.O, "Langmuir, Freundlich, Temkin and Dubinin–Radushkevich Isotherms Studies of Equilibrium Sorption of Zn 2+ Unto Phosphoric Acid Modified Rice Husk," *IOSR J. Appl. Chem.*, vol. 3, no. 1, pp. 38–45, 2012, doi: 10.9790/5736-0313845.

[19]J. N. Wekoye, W. C. Wanyonyi, P. T. Wangila, and M. K. Tonui, "Kinetic and equilibrium studies of Congo red dye adsorption on cabbage waste powder," *Environ. Chem. Ecotoxicol.*, vol. 2, pp. 24–31, 2020, doi: 10.1016/j.enceco.2020.01.004.

[20]H. Al-Zoubi *et al.*, "Comparative adsorption of anionic dyes (eriochrome black t and Congo red) onto jojoba residues: isotherm, kinetics and thermodynamic studies," *Arab. J. Sci. Eng.*, vol. 45, pp. 7275–7287, 2020.

[21]N. F. Al-Harby, E. F. Albahly, and N. A. Mohamed, "Kinetics, isotherm and thermodynamic studies for efficient adsorption of congo red dye from aqueous solution onto novel cyanoguanidine-modified chitosan adsorbent," *Polymers (Basel).*, vol. 13, no. 24, 2021, doi: 10.3390/polym13244446.

[22]C. E. Gimba, A. A. Salihu, J. A. Kagbu, M. Turoti, A. U. Itodo, and A. I. Sariyya, "Study of pesticide (Dichlorvos) removal from aqueous medium by Arachis hypogaea (groundnut shell) using GC/MS," *World Rural Obs.*, vol. 2, no. 1, pp. 1–9, 2010.

[23]N. J. Saleh, M. I. Ismaeel, R. I. Ibrahim, and M. A. Zablouk, "Preparation activated carbon of from Iraqi Reed," *Eng. Technol. J.*, vol. 26, no. 3, 2008.

[24]G. Mckay, *Use of Adsorbents for the Removal of Pollutants from Wastewater*. CRC press, 1995.

[25]S. M. Yakout, A. A. M. Daifullah, S. A. El-Reefy, and H. F. Ali, "Surface modification and characterization of a RS activated carbon: density, yield, XRD, ash, and moisture content," *Desalin. Water Treat.*, vol. 53, no. 3, pp. 718–726, 2015.

[26]T. E. Oladimeji, B. O. Odunoye, F. B. Elehinafe, R. O. Oyinlola, and A. O. Olayemi, "Production of activated carbon from sawdust and its efficiency in the treatment of sewage water," *Heliyon*, vol. 7, no. 1, 2021.

[27]M. Saleem, "Sustainable production of activated carbon from indigenous Acacia etbaica tree branches employing microwave induced and low temperature activation," *Heliyon*, vol. 10, no. 2, 2024.

[28]T. Mkungunugwa, S. Manhokwe, A. Chawafambira, and M. Shumba, "Synthesis and Characterisation of Activated Carbon Obtained from Marula (Sclerocarya birrea) Nutshell," *Journal of Chemistry*, vol. 2021. 2021. doi: 10.1155/2021/5552224.

[29]O. Mohammed, K. Mhamed, and M. Houaria, "Synthesis and characterization of activated carbon from Asphodelus microcarpus in two steps," *Bull. Chem. Soc. Ethiop.*, vol. 38, no. 1, pp. 199–212, 2024.

[30]A. Alhujaily, H. Yu, X. Zhang, and F. Ma, "Adsorptive removal of anionic dyes from aqueous solutions using spent mushroom waste," *Applied Water Science*, vol. 10, no. 7. 2020. doi: 10.1007/s13201-020-01268-2.

[31]E. R. Raut, M. A. Bedmohata, and A. R. Chaudhari, "Study of synthesis and characterization of raw bagasse, its char and activated carbon prepared using chemical additive," *Water Sci. Technol.*, vol. 87, no. 9, pp. 2233–2249, 2023.

[32]A. Aghashiri, S. Hashemian, and F. K. Fotooh, "Adsorption of erochrom black T AzO dye by nanocomposite of activated carbon from sugar beet and LaFeO3," *Desalination and Water Treatment*, vol. 212. pp. 173–184, 2021. doi: 10.5004/dwt.2021.26569.

[33]S. Charafi, F. Z. Janani, A. Elhalil, M. Abdennouri, M. Sadiq, and N. Barka, "Adsorption and Reusability Performances of Ni/Al Layered Double Hydroxide for the Removal of Eriochrome Black T dye," *Biointerface Res. Appl. Chem*, vol. 13, no. 3, 2023.

[34]S. Yadav, A. Yadav, N. Bagotia, N. Sharma, A. K. Sharma, and S. Kumar, "Simultaneous adsorption of three anionic dyes at neutral pH from their individual and multi-component systems on a CTAB modified Pennisetum glaucum based carbon nanotube green composite: Adsorption mechanism and process optimization by Box-Behnken design ," *J. Mol. Liq.*, vol. 358, p. 119223, 2022.

[35]M. S. Manzar *et al.*, "Adsorption behaviour of green coffee residues for decolourization of hazardous congo red and eriochrome black T dyes from aqueous solutions," *Int. J. Environ. Anal. Chem.*, vol. 00, no. 00, pp. 1–17, 2020, doi: 10.1080/03067319.2020.1811260.

[36]Y. Kaur, T. Jasrotia, R. Kumar, G. R. Chaudhary, and S. Chaudhary, "Adsorptive removal of eriochrome black T (EBT)

dye by using surface active low cost zinc oxide nanoparticles: A comparative overview," *Chemosphere*, vol. 278, p. 130366, 2021.
[37]T. A. Aragaw and F. T. Angerasa, "Synthesis and characterization of Ethiopian kaolin for the removal of basic yellow (BY 28) dye from aqueous solution as a potential adsorbent," *Heliyon*, vol. 6, no. 9, 2020.
[38]M. A. Ahmed, M. A. Ahmed, and A. A. Mohamed, "Removal of 4-nitrophenol and indigo carmine dye from wastewaters by magnetic copper ferrite nanoparticles: Kinetic, thermodynamic and mechanistic insights," *J. Saudi Chem. Soc.*, vol. 27, no. 6, p. 101748, 2023.
[39]M. Alamzeb *et al.*, "Kinetic, thermodynamic and adsorption isotherm studies of detoxification of Eriochrome Black T dye from wastewater by native and washed garlic peel," *Water*, vol. 14, no. 22, p. 3713, 2022.

دراسة توازن وثيرموداينميكية لإزالة صبغة Eriochrome Black T من محاليلها المائية باستخدام كربون النانو المحضرة من ساق نبات التوت عبر مرحلتين من الكربونات

ميسون احمد صالح [1*] ، شيرين عثمان اسماعيل [2] ، عماد عبدالاله صالح الحيالى[3]
[1,2]قسم الكيمياء ، كلية العلوم ، جامعة دهوك ، دهوك ، العراق
[3]قسم الكيمياء ، كلية التربية للعلوم الصرفه ، جامعة الموصل ، الموصل ، العراق

الخلاصة:

في هذه الدراسة ، حضر كاربون منشط بحجم النانو (NSAC) باستخدام ساق شجرة التوت ((Morus Nigra (Mulberry) كمادة اولية. تضمنت الدراسة مرحلتين من عملية الكربنة الاولى باستخدام KOH ، تليها معاملة مع هيدروكسيد الصوديوم (NSAC-NAOH) لتعزيز التركيب المسامي الدقيق ،والذي يؤدي إلى زيادة مسامية سطح الكربون المنشط. وقد تم إجراء توصيف شامل للمادة باستخدام تقنيات تحليلية مختلفة ، بما في ذلك التحليل الطيفي للأشعة تحت الحمراء (FT-IR) ، وتحليل Brunauer-Emmett-Teller (BET) ، والمجهر الإلكتروني الضوئي الماسح لمجال الانبعاثات (FE-SEM) ، تشتت التحليل الطيفي للأشعة (EDX) ، وحيود الأشعة السينية (XRD). أظهرت الدراسة وجود حجم الجسيمات على نطاق النانو والمسامية الاستثنائية. علاوة على ذلك ، تم تقييم الخواص الفيزيائية للكربون المنشط. اشتملت الدراسة ايضا على حساب دوال مثل الكثافة والرطوبة ومحتوى الرماد ورقم اليود وسعة امتزاز صبغة المثيلين الزرقاء و والدالة الحامضية عند نقطة صفر (pH_{PZC}). أجريت تجارب الامتزاز في ظل ظروف مثلى ، مع تركيز صبغة Eriochrome Black T (EBT) عند (100 ملغ/لتر) ، وجرعة امتصاصية من (0.4 غم/لتر) ، تركيز أولي (60-110 ملغم/لتر) ،

وعند تسليط الضوء على الدالة الحامضية للمحاليل نجد انه عند (pH=3.0) تظهر اعلى قدرة على إزالة الصبغة المدروسة. لكن بالنظر إلى العوامل الاقتصادية، تم تحديد مستوى الرقم الهيدروجيني الطبيعي ليكون الأمثل للتجارب اللاحقة .وقد أشارت الدراسة الثيرموداينميكية لعملية الامتزاز والتي أجريت ضمن مدى درجات حرارة (25-65 م) ، إلى ان النظام قيد الدراسة ذا طبيعة ماصة للحرارة ($+\Delta H^o$) ،وتدل قيمة التغير في الانثالبي على الامتزاز الفيزيائي المفضل (ΔH^o اقل من 40 كيلوجول/مول). فيما تقترح القيمة السالبة للطاقة الحرة ($-\Delta G^o$) امكانية حدوث الامتزاز بشكل تلقائي. في حين أن قيمة التغير في الانتروبي الإيجابية ($+\Delta S^o$) أشارت إلى زيادة عشوائية النظام بعد عملية الامتزاز. بالإضافة إلى ذلك فقد وجد ان تطبيق النتائج العملية للنظام المدروس عل نموذج ايزوثيرم لا نكماير Langmuir isotherm كان افضل لوصف سلوك الامتزاز لصبغة EBT.